PERGAMON

Journal of Quantitative Spectroscopy & Radiative Transfer 64 (2000) 619–634

Journal of Quantitative Spectroscopy & Radiative Transfer

www.elsevier.com/locate/jqsrt

Diffusion, P_1, and other approximate forms of radiation transport☆

Gordon L. Olson*, Lawrence H. Auer, Michael L. Hall

Transport Methods Group, Los Alamos National Laboratory, P.O. Box 1663, MS D409, Los Alamos, NM 87545, USA

Abstract

Full transport solutions of time-dependent problems can be computationally very expensive. Therefore, considerable effort has been devoted to developing approximate solution techniques that are much faster computationally and yet are accurate enough for a particular application. Many of these approximate solutions have been used in isolated problems and have not been compared to each other. This paper presents two test problems that test and compare several approximate transport techniques. In addition to the diffusion and P_1 approximations, we will test several different flux-limited diffusion theories and variable Eddington factor closures. For completeness, we will show some variations that have not yet appeared in the literature that have some interesting consequences. For example, we have found a trivial way to modify the P_1 equations to get the correct propagation velocity of a radiation front in the optically thin limit without modifying the accuracy of the solution in the optically thick limit. Also, we will demonstrate nonphysical behavior in some published techniques.

Keywords: Time-dependent radiation transport; Diffusion; P_1 approximation; $P_{1/3}$ approximation; Radiation transport; Flux-limited diffusion; Eddington factors

1. Introduction

Many approximate transport techniques have not been adequately tested by making comparisons to analytic solutions. Su and Olson [1] have presented time-dependent nonequilibrium, two temperature, analytic benchmark diffusion and transport solutions that are very useful for testing

☆This work performed under the auspices of the U.S. Department of Energy by Los Alamos National Laboratory under contract W-7405-ENG-36.

* Corresponding author. Tel.: 001-505-667-8105.

E-mail address: glo@lanl.gov (G.L. Olson)

0022-4073/99/$ - see front matter
PII: S0022-4073(99)00150-8

purposes, even though the test problem assumes a constant opacity. This paper introduces a related ideal gas problem that assumes the opacity varies inversely with the cube of the temperature and therefore does not have an analytic solution. These two test problems will be used to test and compare several approximate transport techniques.

The next section presents the equations for several different approximate transport solution techniques. Then in the following two sections these methods are applied to the constant opacity problem of Su and Olson [1] and a variable opacity test problem. Some concluding remarks are given in the last section.

2. Equations for approximate transport models

For simplicity, we will show the equations for radiation transport in only one dimension. All of the techniques discussed here can be generalized to multi-dimensions. The equation for one-dimensional, time-dependent grey transport is

$$\frac{1}{c}\frac{\partial I}{\partial t}+\mu\frac{\partial I}{\partial z}=\kappa B+\frac{c\sigma}{4\pi}E-\chi I=\frac{ac\kappa}{4\pi}T^4+\frac{c\sigma}{4\pi}E-\chi I, \tag{1}$$

where I is the specific intensity, c is the speed of light, t is the time, z is the spatial coordinate, μ is the angle cosine relative to the z-axis, κ is the absorption opacity, σ is the scattering opacity, $\chi=\kappa+\sigma$ is the total opacity, B is blackbody radiation at the local material temperature, T, a is the radiation constant, and E is the radiation energy density. The notation used here follows astrophysical conventions. For more background information and for more details about the physics of transport, see Mihalas [2] for an astrophysical viewpoint or Pomraning [3] or Lewis and Miller [4] for a nuclear engineering viewpoint.

The first three angular moments of I are defined as

$$E=\frac{2\pi}{c}\int_{-1}^{+1}\mathrm{d}\mu I(\mu),\qquad F=2\pi\int_{-1}^{+1}\mathrm{d}\mu\mu I(\mu),\qquad P=\frac{2\pi}{c}\int_{-1}^{+1}\mathrm{d}\mu\mu^2 I(\mu). \tag{2}$$

Where E is the energy density, F is the flux of radiation, and P is the radiation pressure. The zeroth-moment of Eq. (1) is obtained by integrating it over all angles:

$$\frac{1}{c}\frac{\partial E}{\partial t}+\frac{1}{c}\frac{\partial F}{\partial z}=\kappa\left(\frac{4\pi}{c}B-E\right)=\kappa(aT^4-E). \tag{3}$$

Eq. (3) is referred to as the zeroth-moment equation or the energy balance equation.

The first-moment of Eq. (1) is found by multiplying it by μ and then integrating it over all angles to get

$$\frac{1}{c}\frac{\partial F}{\partial t}+c\frac{\partial P}{\partial z}=-\chi F. \tag{4}$$

This equation is the first-moment equation or the momentum balance equation.

Given a material energy balance equation to determine T, Eqs. (3) and (4) have three unknowns: E, F, and P. When dealing with the moments of the transport equation, there is always one more

unknown than there are equations. This is sometimes referred to as the *closure problem*. One needs more information. Different approximation techniques for closing this system of equations are presented in the next few paragraphs. All methods use the same unmodified energy balance equation, Eq. (3).

(a) The P_1 equation can be obtained by setting $P = \frac{1}{3}E$ in Eq. (4). This is the simplest approximation and produces:

$$\frac{1}{c}\frac{\partial F}{\partial t} + \frac{c}{3}\frac{\partial E}{\partial z} = -\chi F. \tag{5}$$

This equation can also be derived by assuming $I(\mu) = I_0 + \mu I_1$, a first-order angular expansion (the first-order Legendre expansion, hence the name "P_1"), and calculating the moments in Eq. (2). Because it allows this linear dependence of the radiation on angle, Morel [5] has shown that in the thick diffusion limit, the P_1 equation has the same zeroth- and first-order expansions as the transport equation. Therefore, the expected behavior of a P_1 solution near the diffusion limit should be reasonably accurate. The main physical disadvantage of the P_1 equation is that in the optically thin limit, with streaming radiation, the propagation velocity is $c/\sqrt{3} = 0.577c$ rather than the correct value of c. This defect will be corrected in subsection (c).

(b) The diffusion equation can be obtained by dropping the time derivative of the flux in the P_1 equation to get

$$\frac{c}{3}\frac{\partial E}{\partial z} = -\chi F \quad \text{or} \quad F = -\frac{c}{3\chi}\frac{\partial E}{\partial z}. \tag{6}$$

Morel [5] has shown that in the diffusion limit this equation is also accurate to first order. Therefore, near the diffusion limit this equation and P_1 should have comparable accuracy. However, in the optically thin limit, this equation has an infinite propagation velocity. Subsection (e) corrects this defect.

(c) Since the P_1 equation in the optically thin limit propagates information too slowly and the diffusion equation propagates it too fast, it seems plausible that one should average these two equations in such a way as to get the correct velocity. It turns out that adding the P_1 equation with a weight of one-third to the diffusion equation with a weight of two-thirds gives the correct propagation velocity. This equation will be called the $P_{1/3}$ equation and is given by

$$\frac{1}{3c}\frac{\partial F}{\partial t} + \frac{c}{3}\frac{\partial E}{\partial z} = -\chi F. \tag{7}$$

Morel [5] has done the diffusion-limit analysis for this equation and found that it has characteristics identical to the P_1 equation. The factor of one-third on the time derivative has corrected the optically thin velocity without decreasing the solution's accuracy in the thick limit. Simmons and Mihalas [6] have found that near the optically thin limit, where there is approximately wave-like propagation, the factor of one-third will cause the wave attenuation to be larger than it should be by a factor of two. However, since the attenuation is small near the wave limit, an error in the attenuation is not as serious as an error in the propagation velocity. It appears that this factor of one-third has provided significant gains without losing anything from the P_1 solution. To our knowledge, Eq. (7) has not appeared anywhere in the literature.

(d) The variable Eddington factor (VEF) equation is given by

$$\frac{1}{c}\frac{\partial F}{\partial t} + c\frac{\partial fE}{\partial z} = -\chi F, \tag{8}$$

where $f = P/E$. The full allowed range for f is $0 \le f \le 1$. If a transport calculation is done to calculate I and its moments in Eq. (2), then f is an accurate representation of the radiation field and the solution of Eq. (8) is an accurate solution of the transport equation. An approximate closure assumes a local function for the Eddington factor. Minerbo [7] has proposed such a closure based on maximum entropy arguments that yield a radiation field of the form $I(\mu) = ae^{b\mu}$. From this expression, the Eddington factor can be calculated as a function of (F/cE). A simple closure suggested by Kershaw [8] is $f = \frac{1}{3} + \frac{2}{3}(F/cE)^2$. All of the proposed local closures interpolate monotonically between the diffusion limit where $f = \frac{1}{3}$ and the streaming limit where $f = 1$. Unfortunately, they therefore exclude an important class of problems where $f < \frac{1}{3}$. More seriously, all local closures cause Eq. (8) to be nonlinear; therefore, feedback in the numerical solution can cause nonphysical radiation "shocks". While the radiation pressure, fE, is continuous, f and E individually can be discontinuous. By averaging f in time and space, these discontinuities can be usually reduced to oscillations in the solution for E. The good news is that with nonlocal VEFs, Eq. (8) is accurate over the full range of optical depths. With local VEFs, Eq. (8) is potentially accurate, but there are no guarantees.

(e) The infinite propagation velocity of the diffusion approximation can be corrected by using a flux-limited diffusion coefficient:

$$F = -cD\frac{\partial E}{\partial z}, \qquad D = \frac{1}{3\chi + \frac{\delta}{E}\left|\frac{\partial E}{\partial z}\right|}, \tag{9}$$

where D is the diffusion coefficient and the form shown here is a generic one usually called the "sum" flux limiter. The factor δ is an adjustable parameter that can be used to try to fit standard test problems, but it is often left at a default value of unity. (In this paper, δ will always be taken as unity.) In the optically thick limit, the gradient of the energy density is small compared to the opacity and this equation reduces to the pure diffusion equation. In the thin limit, the gradient dominates the denominator of D and the flow of radiation is limited to the speed of light, as desired. Unfortunately, a flux-limited diffusion coefficient makes the diffusion equation nonlinear in E. Also, Morel [5] has shown that Eq. (9) is only zeroth-order accurate in the thick limit. Therefore, $I(\mu) = I_0$, an isotropic radiation field, is the best approximation that flux-limited diffusion can make in this limit. As soon as one is slightly away from the thick limit, the solution of Eq. (9) will differ from the transport solution. Because of the structure of the flux limiter, Eq. (9) gets the correct asymptotic limit in the optically thin limit. However, in the process of correcting the thin limit, an order of accuracy in the thick limit has been sacrificed.

(f) Larsen [9] has suggested a modified form for the flux-limited diffusion coefficient that retains first-order accuracy in the thick limit:

$$D = \left[(3\chi)^n + \left(\frac{1}{E}\left|\frac{\partial E}{\partial z}\right|\right)^n\right]^{-1/n}. \tag{10}$$

In the thick limit with $n = 2$, the gradient term is now small *quadratically*; therefore, it does not disturb the linear accuracy of the diffusion solution. With $n > 2$, the gradient term is even smaller.

A related flux limiter is the maximum or "max":

$$D = \frac{1}{\max[3\chi, |\partial E/\partial z|/E]}. \tag{11}$$

This form also retains the linear accuracy of the solution in the thick limit if the opacity term is larger than the gradient term. Unfortunately, this flux limiter has discontinuous derivatives. For large values of n, Eq. (10) approximates Eq. (11) while retaining continuous derivatives.

(g) Levermore and Pomraning [10] (L–P) derived a flux limiter from the transport equation that exactly solved a particular transport problem. They defined some auxiliary functions in addition to a flux limiter:

$$\omega = \frac{\kappa B + \sigma E}{\chi E}, \quad R = \frac{|\nabla E|}{\omega \chi E}, \quad \lambda(R) = \left[\coth(R) - \frac{1}{R}\right]\frac{1}{R}, \quad D = \frac{\lambda(R)}{\omega\chi}, \tag{12}$$

where ω is an albedo, R is a scaled radiation energy density gradient, and $\lambda(R)$ is a function that comes out of their analysis. In the test problems below, this flux limiter will exhibit some nonphysical behavior. Zimmerman [11] suggested the following simplification:

$$\omega = 1, \quad R = \frac{|\nabla E|}{\chi E}, \quad \lambda(R) = \left[\coth(R) - \frac{1}{R}\right]\frac{1}{R}, \quad D = \frac{\lambda(R)}{\chi}. \tag{13}$$

This variation gives much better solutions to the test problems examined here.

(h) One way to get rid of the artificial shocks when using local VEFs is to take the Eddington factor outside of the derivative:

$$\frac{1}{c}\frac{\partial F}{\partial t} + cd\frac{\partial E}{\partial z} = -\chi F. \tag{14}$$

This equation looks like the P_1 equation except that the factor of one-third has been made a variable; therefore, it will be called *variable* P_1 or VP_1. A lower case d has been used to distinguish this coefficient from the diffusion coefficient and the Eddington factor. Note that d has the same range as f in one dimension: $0 \le d \le 1$. Therefore, the same local approximations suggested for f can, potentially, be used for d. However, it is important to note that the only value of d that will cause Eq. (14) to generate an accurate transport solution in a general problem is to use

$$d = \frac{\partial P/\partial z}{\partial E/\partial z} = \frac{\partial P}{\partial E}. \tag{15}$$

Numerically, this ratio of derivatives is much more difficult to calculate than the ratio of moments used to define the Eddington factor. While E is positive, its spatial derivative can change signs causing Eq. (15) to be potentially ill defined when $\partial E/\partial z$ is near zero. Also, d has more spatial structure than f. In our numerical tests, a computational grid that well resolves f in a characteristic ray solution is too coarse to adequately resolve d. Therefore, the use of Eq. (15) does not appear to be practical. To our knowledge, Eq. (14) and its usage has not been published anywhere in the literature. It is presented here as part of a large family of approximations to the transport equation.

(i) For completeness, we present a variation on the previous equations that we do not recommend:

$$\frac{1}{c}\frac{\partial \beta F}{\partial t} + \frac{c}{3}\frac{\partial E}{\partial z} = -\chi F, \tag{16}$$

where $\frac{1}{3} \le \beta \le 1$. Setting $\beta = \frac{1}{3}$ recovers the $P_{1/3}$ equation shown in Eq. (7). However, by making β a variable dependent on the solution, one can attempt to get a more accurate solution. For example, $\beta = 1 - \frac{2}{3}(F/cE)^2$ interpolates between the P_1 and $P_{1/3}$ equations. Unfortunately, this type of local closure makes Eq. (16) nonlinear and can cause numerical instabilities. While the added flexibility of making β a function of E and F may make the numerical solution more accurate in some instances, in general, the improvement over Eq. (7) may not be worth the effort.

(j) Olson and Weaver [12] examined fourth moment closures by coupling the next two higher moment equations to Eqs. (3) and (4). Because the moments of the radiation field are a converging sequence, the solution is less sensitive to the details of how the closure is done when one works with the fourth moment. In one dimension, the four-moment equations can be solved simultaneously as two second-order coupled "diffusion-like" equations. Although the results are not shown here, P_3 and related nonlinear closures at the fourth moment give excellent solutions to the problems in the next two sections. P_3-type solutions are naturally more accurate and they extend to problems where the Eddington factor is less than one-third. Rather than doing considerable work on sophisticated approximate second moment closures, it may be better to use higher-order methods from the beginning.

Summary. Numerically, the diffusion approximations in (b), (e)–(g) are the simplest. The other approximations include the time derivative of the flux; therefore, the value of F must be retained from the previous time step. Using a staggered mesh in one dimension, where the energy densities are at cell centers and fluxes are on cell boundaries, this is trivial. In multi-dimensions, there are several cell faces for each cell center. Therefore, the nondiffusion techniques require more computer storage. However, these fluxes from the previous time step contain important physical information that should improve the accuracy of the nondiffusion solutions.

The methods that keep the flux derivative term in Eq. (4) have a slight numerical advantage when solving the system of equations representing the finite difference equations. The time step increases the effective opacity of a cell by $(c\Delta t)^{-1}$. In optically thin parts of a problem or when the time step is very small, this will decrease the magnitude of the off-diagonal elements of the matrix, thus increasing the diagonal dominance. This change will usually cause iterative solutions of the system of equations to converge slightly faster.

It is instructive to compare the different flux limiters using R, the scaled energy gradient introduced in Eq. (13). Fig. 1 shows five different models for flux limiting. A horizontal line at a value of one-third would represent the case of no flux limiting. The simple sum flux limiter [Eq. (9)] has a value that is too small and limits the flow of radiation too much. The maximum limiter is clearly the least restrictive and will allow the most radiation to flow. Larsen's limiter with $n = 4$ preserves much of the character of the maximum limiter without having a discontinuous derivative.

A surprising fact shown in Fig. 1 is that Larsen's flux limiter with $n = 2$ and the simplified Levermore–Pomraning flux limiter with $\omega = 1$ are almost identical. Derived and proposed from

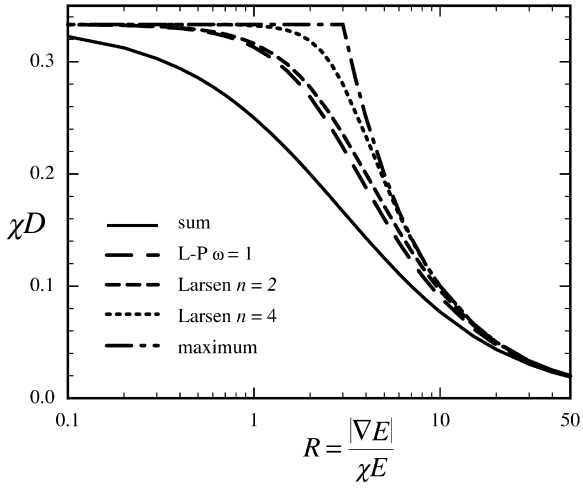

Fig. 1. The scaled diffusion coefficient is shown as a function of a scaled energy gradient. The legend listing the models from top to bottom describes the curves from left to right. L–P refers to the Levermore–Pomraning [10] flux limiter.

very different points of view, the functional forms are very close. In the test problems of the next two sections, these two flux limiters give nearly identical answers. Since the Larsen limiter contains a simple square root function rather than a hyperbolic cotangent, we recommend using Larsen's limiter rather than the simplified Levermore–Pomraning flux limiter. The full L–P limiter in Eq. (12) is too complex to be compared to the other flux limiters in Fig. 1.

3. Constant opacity test problem

Su and Olson [1] defined a basic nonequilibrium radiative transfer problem consisting of an initially cold, homogeneous, infinite, and isotropically scattering medium with an internal radiation source turned on at time zero. While they presented benchmark solutions for problems that include scattering, here we will compare numerical solutions to their pure absorption benchmark. Eq. (1) must be modified to include an isotropic radiation source, S:

$$\frac{1}{c}\frac{\partial I}{\partial t} + \mu\frac{\partial I}{\partial z} = \kappa\left(\frac{ac}{4\pi}T^4 - I\right) + \frac{c}{4\pi}S. \tag{17}$$

Also, an equation describing the exchange of energy between the radiation and material must be specified:

$$\frac{C_V}{c}\frac{\partial T}{\partial t} = \kappa(E - aT^4), \tag{18}$$

where C_V is the heat capacity of the material, assumed to be proportional to the cube of the material temperature, $C_V = \alpha T^3$. This assumption is based on mathematical convenience rather than physical correctness. Inserting this assumption into Eq. (18) and rearranging gives an

equation that is linear in T^4:

$$\frac{\alpha}{4c}\frac{\partial T^4}{\partial t} = \kappa(E - aT^4). \tag{19}$$

By also assuming that the opacity was a constant, Su and Olson [1] were able to obtain a closed-form solution for scaled variables of the material temperature to the fourth power and radiation energy density

$$\theta \equiv \hat{T}^4 \equiv \left(\frac{T}{T_{\mathrm{H}}}\right)^4 \quad \text{and} \quad \hat{E} \equiv \frac{E}{aT_{\mathrm{H}}^4} \equiv \left(\frac{T_{\mathrm{r}}}{T_{\mathrm{H}}}\right)^4 \equiv \hat{T}_{\mathrm{r}}^4, \tag{20}$$

where T_{H} is a Hohlraum or reference temperature and T_{r} is the radiation temperature. Using these new variables and introducing a scaled time variable, one can rewrite the material energy balance equation as

$$\frac{\alpha}{4ac\kappa}\frac{\partial \hat{T}^4}{\partial t} = \hat{E} - \hat{T}^4, \tag{21}$$

or

$$\frac{\partial \theta}{\partial \tau} = \hat{E} - \theta \quad \text{where } \tau \equiv \frac{4ac\kappa}{\alpha}\, t. \tag{22}$$

Rewriting Eq. (17) with these scaled variables and a scaled radiation intensity gives

$$\frac{4a}{\alpha}\frac{\partial \hat{I}}{\partial \tau} + \frac{\mu}{\kappa}\frac{\partial \hat{I}}{\partial z} = \left(\frac{\theta}{4\pi} - \hat{I}\right) + \frac{S}{4\pi\kappa aT_{\mathrm{H}}^4}, \tag{23}$$

where

$$\hat{I} \equiv \frac{I}{caT_{\mathrm{H}}^4}. \tag{24}$$

The zeroth- and first-angular moments of this scaled equation are

$$\frac{4a}{\alpha}\frac{\partial \hat{E}}{\partial \tau} + \frac{1}{\kappa}\frac{\partial \hat{F}}{\partial z} = \theta - E + \frac{S}{\kappa aT_{\mathrm{H}}^4}, \tag{25}$$

$$\frac{4a}{\alpha}\frac{\partial \hat{F}}{\partial \tau} + \frac{1}{\kappa}\frac{\partial \hat{P}}{\partial z} = -\hat{F}, \tag{26}$$

where

$$\hat{F} \equiv \frac{F}{caT_{\mathrm{H}}^4}, \quad \hat{P} \equiv \frac{P}{aT_{\mathrm{H}}^4}. \tag{27}$$

Eqs. (21)–(26) simplify significantly if one chooses $\alpha = 4a$, i.e., $C_V = 4aT^3$, and $\kappa = 1$. With these choices the time variable becomes $\tau = ct$. The tables for the analytic solution in space and time given by Su and Olson [1] use these values and

$$\hat{S} \equiv \frac{S}{aT_{\mathrm{H}}^4} = 1 \quad \text{for } |z| \le \frac{1}{2} \quad \text{and} \quad ct \le 10 \quad \text{elsewhere } \hat{S} = 0. \tag{28}$$

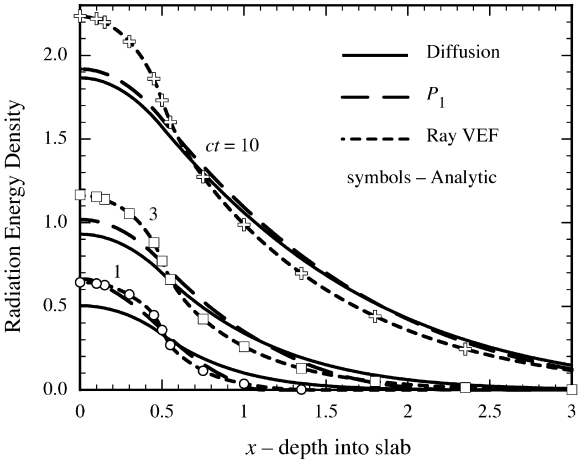

Fig. 2. The analytic benchmark solution of Su and Olson [1] (symbols) is compared to diffusion, P_1, and a characteristics ray Eddington factor solutions on a linear scale.

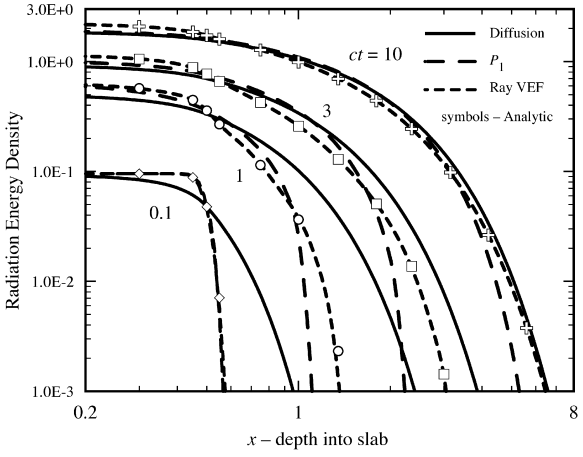

Fig. 3. Same as in Fig. 2 except it is on a logarithmic scale.

At the midplane, $z = 0$, a symmetry boundary condition is applied so that the calculational space is $0 \le z \le 30$. The radiation does not travel from the source region to the boundary at $z = 30$ in the time of interest. At $z = 30$ we use a fixed-temperature boundary condition of $\theta(30,t) = \hat{E}(30,t) = 10^{-10}$, which is also the initial value, $\theta(x,0) = \hat{E}(x,0) = 10^{-10}$.

Figs. 2 and 3 compare diffusion, P_1, and a transport Eddington factor solution to the benchmark solution of Su and Olson [1]. For the Eddington factor solution, time-dependent solutions of Eq. (17) along rays passing through the slab were done at standard Gaussian quadrature angles. Only eight angles were required to accurately compute the Eddington factor, $f = P/E$, that was then used in the moment equations. In the figures, the variable Eddington factor solution goes through the symbols for the analytic solution. The diffusion solution without any flux limiter propagates radiation out ahead of the transport solution in Fig. 3, while P_1 lags behind the transport solution. Near $x = 0$ in Fig. 2, neither P_1 nor diffusion match the transport solution very well at $ct = 3$ or 10. From Fig. 3, it is clear that early in time, near a boundary layer, P_1 is significantly better than diffusion.

Fig. 4 compares three different flux-limited diffusion solutions to the benchmark solution. The sum flux limiter looks good early in time but it lags significantly behind the transport solution as it approaches the equilibrium solution at depth. The maximum flux limiter's solution has a noticeable bend in the solution at time $ct = 1$ and $x = 1.5$. The discontinuous derivative of the limiter is apparent at this point. Larsen's flux limiter using $n = 2$ gives the best solutions at $ct = 3$ and 10, and it is well behaved early in time. The Levermore–Pomraning simplified flux limiter with the albedo set to unity gives a solution (not shown) that is just very slightly to the left of the Larsen solution.

Fig. 5 shows the $P_{1/3}$ solution, a variable Eddington factor solution using Minerbo's [7] prescription for a local closure, and diffusion using the full Levermore–Pomraning [10] diffusion coefficient. The $P_{1/3}$ solution tracks the position of the wave front well and gives a smooth

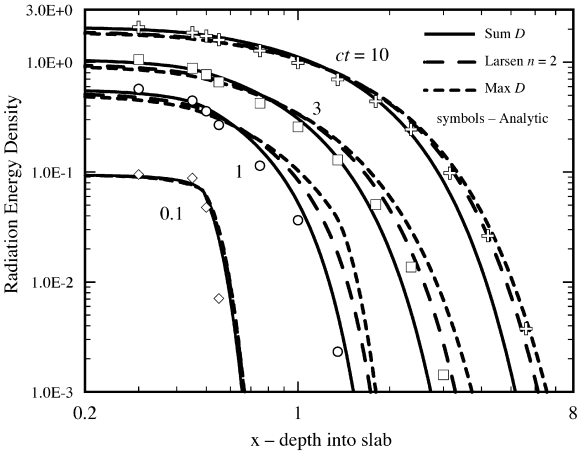

Fig. 4. Same as in Fig. 3 except it is for three diffusion flux limiters: the sum, maximum, and Larsen (with $n = 2$) limiters.

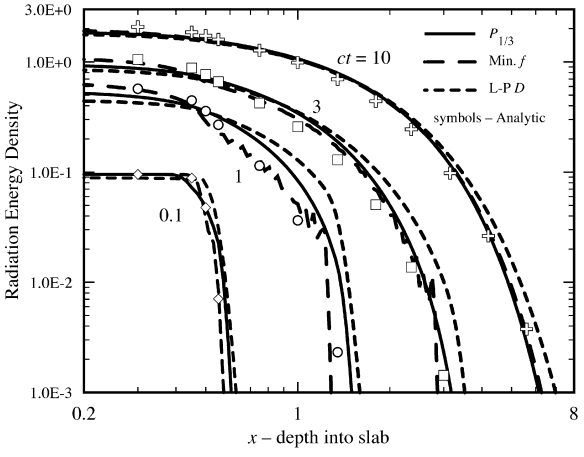

Fig. 5. Same as in Fig. 3 except it is for $P_{1/3}$, Minerbo [7] local variable Eddington factor, and Levermore–Pomraning [10] flux-limited diffusion solutions.

well-behaved answer. As discussed in the previous section, local Eddington factor closures are numerically unstable and give a noisy solution. At $ct = 10$, the solution becomes smooth as it transitions to the equilibrium diffusion solution. The Levermore–Pomraning flux limiter gives a good solution for the early time steps, but at $ct = 10$, it produces a nonphysical result by allowing energy ahead of the nonflux limited solution shown in Fig. 3.

Fig. 6 presents the Eddington factors for the characteristic ray solution, shown in Figs. 2 and 3, and the Minerbo local closure of Fig. 5. On this linear plot, the noise in the local closure looks even worse than in Fig. 5. Note that the accurate solution shows Eddington factors in the source region are significantly below one third, while the local closure has the built in assumption that the correct range is $\frac{1}{3} \leq f \leq 1$. This discrepancy indicates why all the approximate theories fit the transport solution so poorly near $x = 0$ in Fig. 2. None of the approximate theories allow for $f \leq 1/3$.

Fig. 6 also indicates why the Levermore–Pomraning flux limiter produced a nonphysical result. In their paper, Levermore and Pomraning, [10], introduced a normalized specific intensity, $\psi(z, \mu, t) \equiv I(z, \mu, t)/cE(z, t)$. Then in parts of the derivation they assumed that this normalized specific intensity was slowly varying in space and time. This normalization removes the rapid variation in space and time near a wave front. However, the angular dependence also rapidly varies near a wave front. The Eddington factor, being the ratio of the second angular moment to the zeroth angular moment, is a good measure of the angular-dependent part of the radiation field. Clearly from Fig. 6, near a wave front the Eddington factor does not vary slowly. Therefore, the derivation's assumptions break down precisely where the flux limiter is most needed, at a wave front. This nonphysical behavior of propagating a wave front faster than the nonflux-limited solution is worse in the problem of the next section.

Fig. 7 shows the results of using the methods discussed in subsections (h) and (i) and using Levermore's [13] suggestion for a local closure for a VEF. The methods of (h) and (i) have nothing to distinguish them from the other techniques. Several different approximations were used for

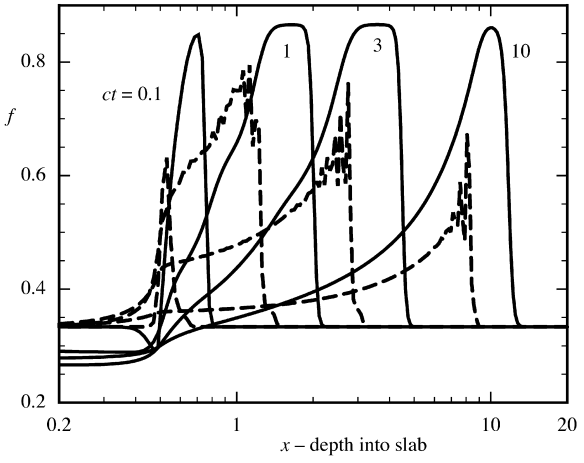

Fig. 6. The variable Eddington factors for the characteristic ray solution (solid lines) and for the Minerbo local approximate closure (dashed lines).

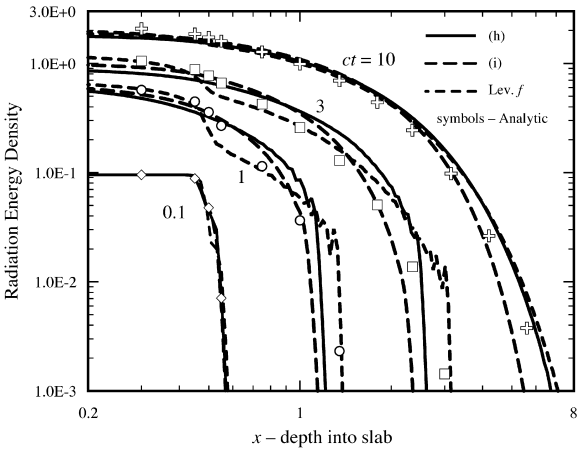

Fig. 7. Same as in Fig. 3 except it is for Levermore [13] variable Eddington factor and the methods in subsections (h) and (i).

d and ω, but none of them gave significantly better results than the other methods. Levermore's VEF [13] suffers from the same problems as Minerbo's VEF [7] shown in Fig. 5.

4. Variable opacity test problem

The test problem of the previous section is useful because Su and Olson [1] were able to obtain exact solutions (to four significant digits). Unfortunately, the assumption of constant opacity is not realistic and therefore the comparisons made in the last section cannot be considered definitive. Therefore, we propose a related problem where the opacity varies inversely with the cube of the temperature, $\kappa = \kappa_0 \hat{T}^{-3} = \kappa_0 \theta^{-3/4}$, and the heat capacity is a constant. In this problem the opacity has physically reasonable temperature dependence while the heat capacity is that of an ideal gas. The advantage of this choice is that the material energy balance equation is simple and will look almost identical to Eq. (22) in the previous section with a slightly redefined time variable:

$$\frac{C_V}{4c\kappa_0 T_{\mathrm{H}}^3}\frac{\partial T^4}{\partial t} = E - aT^4, \tag{29}$$

or

$$\frac{\partial \theta}{\partial \tau} = \hat{E} - \theta \quad \text{where } \tau \equiv \frac{4ac\kappa_0 T_{\mathrm{H}}^3}{C_V} t. \tag{30}$$

The transport equation and its angular moments in terms of normalized variables now must include the nonlinear opacity:

$$\varepsilon \frac{\partial \hat{I}}{\partial \tau} + \frac{\mu}{\kappa_0}\frac{\partial \hat{I}}{\partial z} = \theta^{-3/4}\left(\frac{\theta}{4\pi} - \hat{I}\right), \tag{31}$$

$$\varepsilon \frac{\partial \hat{E}}{\partial \tau} + \frac{1}{\kappa_0} \frac{\partial \hat{F}}{\partial z} = \theta^{-3/4}(\theta - \hat{E}), \tag{32}$$

$$\varepsilon \frac{\partial \hat{F}}{\partial \tau} + \frac{1}{\kappa_0} \frac{\partial \hat{P}}{\partial z} = -\theta^{-3/4}\hat{F}, \tag{33}$$

where

$$\varepsilon \equiv \frac{4aT_{\mathrm{H}}^3}{C_V} \quad \text{and} \quad \tau = \varepsilon\kappa_0 ct. \tag{34}$$

These equations are clearly nonlinear because of the variable opacity; therefore, the technique used by Su and Olson to get an analytic solution is not applicable. However, as in the previous section we choose $\varepsilon \equiv 1$ ($C_V = 4aT_{\mathrm{H}}^3$) and $\kappa_0 = 1$. Then time is scaled by the speed of light, $\tau = ct$. If one prefers to use $\kappa_0 \neq 1$, then one can introduce a scaled spatial variable, $x \equiv \kappa_0 z$, and interpret the results below in terms of this scaled variable. Because the opacity was specified in normalized temperature units, one must also use $T_{\mathrm{H}} \equiv 1$, in order that everyone agrees what the opacity function is.

Instead of an internal source term, for this problem we will apply an isotropic radiation field incident on the slab's surface at $z = 0$:

$$I(\mu, 0, t) = B(T) = \frac{ac}{4\pi} T_{\mathrm{H}}^4 \quad \text{or} \quad \hat{I}(\mu, 0, \tau) = \frac{1}{4\pi}. \tag{35}$$

In order to apply this type of boundary condition to the moment equations, we need to relate the intensity self-consistently to its moments. If one assumes $I(z, \mu, t) = I_0(z, t) + \mu I_1(z, t)$ and integrates the zeroth- and first-angular moments of this linear expansion, then I_0 and I_1 can be related to E and F:

$$I(z, \mu, t) = \frac{cE(z, t)}{4\pi} + \mu \frac{3F(z, t)}{4\pi}. \tag{36}$$

Then integrating the boundary condition over the half range in angle gives

$$\begin{aligned} F^{\mathrm{inc}}(0, t) &= 2\pi \int_0^1 B(T)\mu \, \mathrm{d}\mu = \pi B(T) = \frac{ac}{4} T_{\mathrm{H}}^4 = \frac{c}{4} E_{\mathrm{H}} \\ &= 2\pi \int_0^1 \left(\frac{cE(0, t)}{4\pi} + \mu \frac{3F(0, t)}{4\pi} \right) \mu \, \mathrm{d}\mu = \frac{c}{4} E(0, t) + \frac{1}{2} F(0, t). \end{aligned} \tag{37}$$

This is usually referred to as a Marshak boundary condition. It is used by solving for F and using it in the flux continuity equation for one side of the first cell in the slab:

$$F(0, t) = 2F^{\mathrm{inc}}(0, t) - \frac{c}{2} E(0, t), \tag{38}$$

or

$$\hat{F}(0, \tau) = \tfrac{1}{2} - \tfrac{1}{2}\hat{E}(0, \tau). \tag{39}$$

The initial condition for the cold slab is to use $\hat{E}(x,0) = \theta(x,0) = 10^{-5}$ or $\hat{T}(z,0) = 10^{-1.25} = 0.05623$

The normalized equations (32) and (33) are relatively simple when one chooses $\varepsilon \equiv 1$ and $\kappa_0 \equiv 1$. These equations can be related to real codes with nonnormalized variables by taking an ideal gas as an example. For an ideal gas, the heat capacity is given by the density times the specific heat, which is known in terms of atomic constants:

$$C_V = \rho c_V = \frac{3}{2}\frac{\rho k}{m}, \tag{40}$$

where m is the mass of a hydrogen atom and k is the Boltzmann constant. In order to get $\varepsilon \equiv 1$, one must have

$$T_{\mathrm{H}}^3 = \frac{C_V}{4a} = \frac{3\rho k}{8ma}. \tag{41}$$

Therefore, in a high-temperature plasma code that uses "temperatures" in keV, $T_{\mathrm{H}} = 1$ keV, and the appropriate mass density is 0.38214 g cm^{-3}. This is a little cooler and less dense than at our sun's center.

In other papers, some authors have studied a problem nearly identical to the one proposed in this section; however, they set $\kappa_0 = c = a = 1$. Such a choice is reasonable for idealized test codes; however, it is difficult for codes with real physics to make such arbitrary changes. Therefore, it is hoped that the problem as scaled here will be easier for physics codes to calculate.

The finite difference forms of Eqs. (25) and (26) in the previous section and Eqs. (32) and (33) in this section have E, f, and P at cell centers and F, D, and d on cell edges. θ in Eqs. (30) and (32) is evaluated at the cell center temperature, while θ in Eq. (33) is evaluated at the cell edge temperature which is taken to be the average of the two neighboring cell centers. Similarly, the diffusion coefficients, D, are evaluated at the cell edge temperatures. Because of the nonlinearity of the opacities it is important to average the temperatures rather than average the opacities. Also, it is necessary either to iterate for the solution at the new time step with implicit opacities or to use a very small time step. Otherwise the numerical solution will drift away from the correct spatially and temporally resolved solution.

Fig. 8 shows the radiation and material temperatures as the Marshak wave penetrates into the slab. Because of the temperature-dependent opacity, the front of the wave stays sharp, it does not spread out significantly as it propagates.

Fig. 9 compares many different methods at one time ($ct = 30$) with a greatly expanded spatial scale. The "exact" solution is the second curve from the left. While there is no analytic solution to this nonlinear problem, this solution is the converged answer arrived at with two completely different methods: characteristic rays calculating VEFs and P_N from the Spartan package by Michael Hall. The two methods converged with six angles for calculating the Eddington factor and at P_5, respectively. This problem does not require high angle quadrature. As mentioned earlier, P_3 gives a quite adequate solution.

From Fig. 9, it is clear that the sum flux limiter slows down the wave propagation too much. The L–P flux limiter is the rightmost curve and is significantly out ahead of the nonflux-limited solution. As discussed earlier, the approximations made in deriving this limiter are not correct near

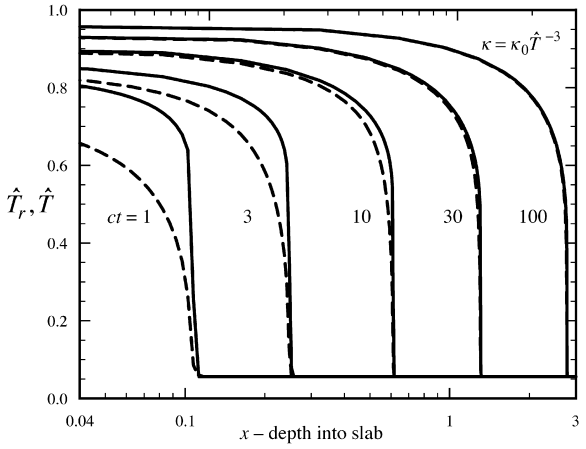

Fig. 8. The normalized radiation (solid lines) and material (dashed lines) temperatures are shown as a function of space at different times for the temperature-dependent opacity problem.

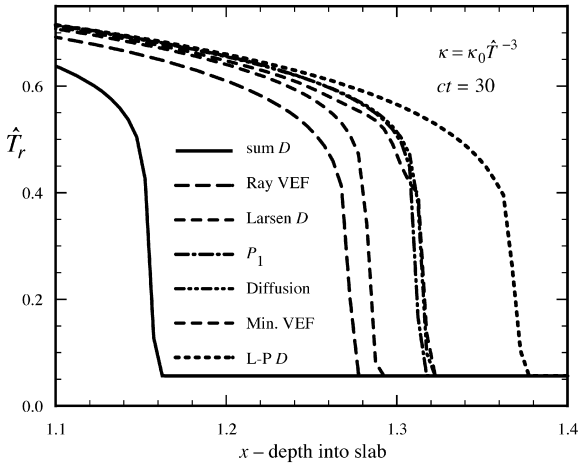

Fig. 9. The normalized radiation temperature is shown as a function of space at one time for several different approximate transport models. The models listed top to bottom are in the left to right order at $T_r = 0.2$.

a sharp wave front. The solution with Larsen's $n = 2$ flux limiter is the one closest to the transport solution in this problem. The solution with the simplified L–P limiter with $\omega = 1$ (not shown) would be just slightly to the left of the curve for Larsen's limiter. The three curves grouped very close together are P_1, diffusion, and Minerbo's local VEF. In this problem, P_1 propagates only slightly slower than diffusion, the difference is almost negligible. The local VEF solution is just below the P_1 solution until right at the wave front where it has a bend and then goes in front of the diffusion solution. The large opacity changes have dampened the oscillations that occurred in the local VEF solutions of the constant opacity problem. Not shown is the $P_{1/3}$ solution because it lies between the P_1 and diffusion solutions. The "max" flux limiter solution is also not shown as it is identical to the nonflux-limited diffusion solution.

Although Larsen's $n = 2$ flux limiter gives the solution closest to transport in this problem, that does not mean that it is the best in any other problem. This limiter gives a smooth transition from diffusion to the streaming limits without reducing the accuracy of the diffusion limit. That is how it was chosen. It has no sophistication or transport knowledge. In the constant opacity problem, this limiter and the $P_{1/3}$ solution are almost identical. We prefer the $P_{1/3}$ method as more general purpose because it does not throw away the flux derivative term and then introduce an ad hoc limiter to repair the damage done by throwing away some physics.

In passing, we draw the reader's attention to the fact that, even though the wave front is deep into the material and the optical depth ahead of the wave front is several thousand, there are still important differences between diffusion and transport. Simply being optically thick is not sufficient to assure the validity of the diffusion limit. The sharp edge at the front of the wave acts as an internal boundary, the structure of which neither diffusion nor P_1 can accurately model.

5. Conclusions

This paper has compared several approximate transport methods to each other and to full transport in two test problems. Flux-limited diffusion using the simple sum flux limiter of Eq. (9) is perhaps one of the most common approximations and it is also one of the least accurate. This limiter restricts the flow of radiation too much and Morel's [5] analysis shows that it results in a solution that is only zeroth-order accurate in the diffusion limit. The only reason to use this limiter is for a crude estimation of the size of transport effects. If a solution with the sum limiter differs drastically from one using the better limiters, then a full transport calculation may differ significantly from any of the diffusion solutions.

The Levermore–Pomraning flux limiter should not be used for the class of problems presented here. If the problem being solved is very similar to the problem for which the L–P limiter gives the exact solution [10], then it is an appropriate choice. The nonphysical behavior of pushing radiation out ahead of the nonflux-limited solution makes this limiter unreliable for some classes of problems. The simplified form using $\omega = 1$ gives better results, but it is so close to Larsen's $n = 2$ limiter, that it does not need to be used.

Of the flux-limited diffusion schemes, Larsen's $n = 2$ limiter is the recommended choice. It is the simplest limiter that has all the desired properties. The solution near the diffusion limit agrees with the transport solution to first order when n is greater than or equal to 2. By comparing the different solutions using $n = 1$, 2, and 4, one can *perhaps* crudely estimate whether a full transport calculation is required. If all three results are identical, transport may be unnecessary.

The $P_{1/3}$ method is a corrected form of P_1 that has the correct propagation velocity in the optically thin limit. Unlike flux-limited diffusion, this is a linear closure that does not throw away the flux derivative term in the momentum balance equation. It should be pointed out that flux-limited diffusion couples the wrong momentum to the material that the radiation is flowing through. Therefore, $P_{1/3}$ is recommended over any of the flux-limited diffusion theories as a general-purpose choice.

Local closures using variable Eddington factors (VEF) are not recommended. This method gives nonsmooth solutions that are not any better than the other techniques.

Nonlocal VEFs can give transport accurate results if the angle and spatial zoning are converged. These solutions were presented here as the transport solutions the approximate theories were striving to match. A potentially fruitful area of future research is to determine how to maximize the accuracy of nonlocal VEFs while minimizing the computational work in multi-dimensional geometries.

It must be emphasized that the thorough testing of new closures and approximate theories is absolutely essential. While not exhaustive, the two problems used here are complementary in how they test-proposed algorithms and the codes written with those algorithms. The first one tests optically thin and boundary layer behavior. The temperature-dependent opacity in the second problem provides a stringent test of zoning and time step control in addition to transport effects. Whenever possible, one should do a transport calculation of a realistic and relevant problem and compare the approximate solutions to the transport answer.

The comparisons presented in this paper are limited to one dimension. The performance of the different approximations and their relative merits may change significantly when issues of complex geometries in multi-dimensions are important.

References

[1] Su B, Olson GL. Ann Nucl Energy 1997;24:1035–55.
[2] Mihalas D. Stellar atmospheres. San Francisco, CA: W.H. Freeman & Co, 1978.
[3] Pomraning GC. The equations of radiation hydrodynamics. Oxford: Pergamon Press, 1973.
[4] Lewis EE, Miller WF. Computational methods of neutron transport. La Grange Park, IL, USA: ANS Inc., 1993.
[5] Morel JE. Asymptotic accuracy of diffusion, P_1, and flux-limited diffusion theories in the equilibrium-diffusion limit. JQSRT 1999; this volume.
[6] Simmons KH, Mihalas D. A linearized analysis of the modified P_1 equations. JQSRT 1999; this volume.
[7] Minerbo GN. JQSRT 1978;20:541.
[8] Kershaw DS. Flux limiting nature's own way. Lawrence Livermore National Laboratory, UCRL-78378, 1976.
[9] Larsen E. 1998, private communication.
[10] Levermore CD, Pomraning GC. Astrophys J 1981;248:321.
[11] Zimmerman G. 1998, private communication.
[12] Olson GL, Weaver RP. One-dimensional photon transport: variable eddington factors and higher moment expansions. LA-UR-84-3636, Los Alamos National Laboratory, 1984.
[13] Levermore CD. A Chapman-Enskog approach to flux-limited diffusion theory. Lawrence Livermore National Laboratory, UCID-18229, 1979.